

See discussions, stats, and author profiles for this publication at: <https://www.researchgate.net/publication/231429428>

# Fluorescence quenching by counterions in ionic micelle solution. The effect of ion migration

ARTICLE in THE JOURNAL OF PHYSICAL CHEMISTRY · JANUARY 1984

Impact Factor: 2.78 · DOI: 10.1021/j150646a025

---

CITATIONS

38

---

READS

17

5 AUTHORS, INCLUDING:



Mats Almgren

Uppsala University

212 PUBLICATIONS 9,653 CITATIONS

SEE PROFILE



Mark Van der Auweraer

University of Leuven

333 PUBLICATIONS 8,388 CITATIONS

SEE PROFILE



Frans C De Schryver

University of Leuven

669 PUBLICATIONS 21,107 CITATIONS

SEE PROFILE

# Fluorescence Quenching by Counterions in Ionic Micelle Solution. The Effect of Ion Migration

M. Almgren,\*

*Institute of Physical Chemistry, University of Uppsala, S-75121 Uppsala, Sweden*

P. Linse,

*Physical Chemistry I, Chemical Center, S-22007 Lund 1, Sweden*

M. Van der Auweraer, F. C. De Schryver, E. Geladé, and Y. Croonen

*Department of Chemistry, K. U. Leuven, Celestijnenlaan 200 F, B 3030 Heverlee, Belgium*

*(Received: April 28, 1983)*

The Poisson-Boltzmann (PB) equation was solved numerically in the cell model to yield the electrostatic potential of a model micelle solution. The system was chosen to mimic a solution of sodium dodecyl sulfate (SDS). Mean first passage times (MFPTs) were then calculated for the diffusion of bivalent and univalent cations, and neutral species, according to some different prescriptions in the cells. The concept of binding is discussed, in particular how it implicitly enters the current kinetic description of fluorescence quenching by counterionic quenchers in micelle solution. It is shown that in the case of multivalent quencher ions, moving among the univalent counterions of the micelle, almost all quenchers must in practice be regarded as bound. The residence time of the quencher with a particular micelle decreases rapidly with micelle concentration, in accord with experimental observation. Also for univalent quencher ions the "kinetic" definition of binding yields a much larger fraction of bound ions than spectroscopic or thermodynamic definitions.

## Introduction

The quenching of fluorescence in micelle solutions has been studied extensively. As far as hydrophobically bound substances are involved, it is well understood.<sup>1-4</sup> A quite general theory (eq 1) for the observed fluorescence decay after  $\delta$ -pulse excitation at  $t = 0$  was suggested<sup>1</sup> and derived<sup>2</sup> early, and was later extended somewhat to account for static quenching<sup>5</sup> and polydispersity effects.<sup>6</sup>

$$\begin{aligned} F(t) &= A_1 \exp(-A_2 t - A_3(1 - \exp(-A_4 t))) \\ A_1 &= F(0) \\ A_2 &= k_0 + k_-(x)k_q/(k_q + k_-) \\ A_3 &= \langle x \rangle [k_q/(k_q + k_-)]^2 \\ A_4 &= k_q + k_- \end{aligned} \quad (1)$$

where  $k_0 = 1/\tau_0$  is the deactivation rate constant of the fluorescent probe in the absence of quenching,  $k_q$  the first-order rate constant of quenching in a micelle with one quencher,  $k_-$  the exit rate constant for a quencher from a micelle and  $\langle x \rangle$  the average number of quenchers per micelle. Details of the derivation of eq 1 are found in ref 1 and 2. An important assumption is that  $k_-$  and the entrance rate constant  $k_+$  both are independent of the number of quenchers in the micelle. This assumption implies Poisson statistics for the distribution of quenchers on the micelles.

When one assumes that  $k_q \gg k_-$ , i.e., that quenching occurs rather than escape, the parameters in eq 1 are considerably simplified and their physical meaning is clearly seen. The second term in the exponent is related to the rapid quenching in micelles that contained quenchers at  $t = 0$ , whereas the fraction  $\exp(-\langle x \rangle)$  of micelles was without quenchers at  $t = 0$  and gives an exponential fluorescence decay with decay constant  $A_2 = k_0 + k_-(x)$ . The

second term here is from the quenching by quenchers diffusing to the micelle, as seen from the equilibrium condition

$$k_-(x) = k_+[Q]_{aq} \quad (2)$$

where  $[Q]_{aq}$  is the concentration of free quenchers.

When a kinetic analysis based on eq 1 and 2 was applied to the quenching of pyrene fluorescence in anionic micelles by metal ions, an inconsistency was revealed in that  $k_-$  and  $k_+$  were found to depend on the micelle concentration.<sup>7,8</sup> It was later shown by some numerical calculations based on computer solutions of the Poisson-Boltzmann equation that a strongly increasing rate of ion migration with increasing micelle concentration is to be expected, which explains the findings.<sup>9</sup>

However, there are several questions concerning the applicability of the quenching model expressed by eq 1 and 2 to ionic quenchers which were left unanswered and even unaddressed in the previous papers. These questions are related to the concept of ion binding and to the physical meaning of the rate parameters  $k_-$ ,  $k_+$ , and  $k_q$  in charged systems.  $k_-$  and  $k_q$  are rate constants giving escape frequency and reaction frequency for quencher molecules "bound" to the micelles; the application of eq 1 and 2 therefore requires a clear definition of the binding concept. The meaning of this concept will be examined for ionic quenchers bound only electrostatically. A comparison of calculated and experimental  $k_-$  values for  $\text{Cu}^{2+}$  will be made over a wide concentration range of sodium dodecyl sulfate (SDS) micelles.

## Definition of Binding and Rate Constants

Equation 1 may be regarded as an appropriate solution to a diffusional fluorescence quenching problem, displaying a transient and a steady-state phase. The transient phase is greatly amplified by the presence of the micelles which effectuate that a large fraction of the excitations occur close to quenchers. The steady-state part is controlled by diffusion, in the appropriate potential, of the quenchers to the micelle surface. The detailed time dependence in the initial phase will not be discussed. It can only be predicted on the basis of a detailed model regarding

- (1) Infelta, P. P.; Grätzel, M.; Thomas, J. K. *J. Phys. Chem.* **1974**, *78*, 190.
- (2) Tachiya, M. *Chem. Phys. Lett.* **1975**, *33*, 289.
- (3) Löfroth, J.-E.; Almgren, M. *J. Chem.* **1982**, *86*, 1636.
- (4) Croonen, Y.; Geladé, E.; Van der Zegel, M.; Van der Auweraer, M.; Vandendriessche, H.; De Schryver, F. C.; Almgren, M. *J. Phys. Chem.* **1983**, *87*, 1426.
- (5) Van der Auweraer, M.; Dederen, J. C.; Geladé, E.; De Schryver, F. C. *J. Chem. Phys.* **1980**, *74*, 1140.
- (6) Almgren, M.; Löfroth, J. E. *J. Chem. Phys.* **1982**, *76*, 2734.

- (7) Dederen, J. C.; Van der Auweraer, M.; De Schryver, F. C. *Chem. Phys. Lett.* **1979**, *68*, 451; *J. Phys. Chem.* **1981**, *85*, 1198.
- (8) Grieser, F.; Tausch-Treml, R. *J. Am. Chem. Soc.* **1980**, *102*, 7258.
- (9) Almgren, M.; Gunnarsson, G.; Linse, P. *Chem. Phys. Lett.* **1982**, *85*, 451.

distribution, reaction, and diffusion in the reaction zone.<sup>5,10-12</sup> We will only assume that the quenching is fast and the binding strong so that a quencher will very rarely escape a micelle leaving an excited probe behind. The steady-state process is then from eq 1

$$F(t)/F(0) = \exp[-A_3 - A_2t] \quad (3)$$

It is described by only two parameters: an amplitude,  $\exp(-A_3)$ , which gives the fraction of excitations that occurred in micelles without bound quenchers, and the decay constant  $A_2$ , which is the sum of the fluorescence decay constant  $k_0$  and the rate of arrival of quenchers to the micelle by steady-state diffusion.

Thus, the quenching process singles out those quenchers that are at a micelle surface or in its vicinity. It is inevitable that these will be regarded as bound. For strongly bound neutral quenchers the definition selects indeed those quenchers that are solubilized by the micelles. In the ionic case, however, at  $t = 0$  an appreciable fraction of the quenchers may be outside the reaction zone surrounding the micelle surface and still take part in the transient phase of the quenching. The probability for this to happen will depend on the initial location of the quencher, being close to unity in the reaction zone and close to zero when the quencher is caught by the field of a neighbor micelle. If the transition from unity to zero occurs in a narrow range of  $r$  values, then the midpoint of the transition range will give an approximate delimitation of where bound quenchers are found.

A complete solution of the Smoluchowski equation for a specified model is required in an analysis along these lines. We will not attempt that here, but instead investigate how the mean first passage time,  $\tau(r_0, r_m)$  (Appendix B) for a quencher for going from  $r_0$  to the micelle surface and  $\tau(r_0, r_c)$  from  $r_0$  to the cell boundary, varies with  $r_0$ . A rapid transition from a region where  $\tau(r_0, r_m)$  is much larger than  $\tau(r_0, r_c)$  to one where the opposite is true would indicate the feasibility of a bound-free subdivision. A delimitation of the bound region would then be given by  $r_b$  such that

$$\tau(r_b, r_m) = \tau(r_b, r_c) \quad (4)$$

It is also necessary to inquire whether a condition corresponding to  $k_q \gg k_-$  for neutral quenchers holds.  $k_q$  and  $k_-$  are quenching frequency and escape frequency for a bound quencher. With a quenching frequency of  $k_q'$  in the reaction zone, we have

$$k_q = P_r k_q' \quad (5)$$

where  $P_r$  is the probability that the bound quencher is also in the reaction zone. The escape rate constant is equal to the inverse of the mean residence time in the bound state, which is given by  $\tau(r_0, r_c)$  averaged over an equilibrium distribution of start positions in the bound region. With the exception of resonance energy transfer, the quenching processes require a molecular encounter between probe and quencher. The quenching frequency is therefore at most diffusion limited. A comparison of the residence time with the mean time required for a quencher to diffuse a length equal to the circumference of the micelle is then of relevance.

The concept of bound ions proposed here is quite different from those normally discussed.<sup>13,14</sup>

Lindman and Wennerström<sup>14</sup> distinguish three different kinds of measurements to determine ion binding. Spectroscopic measurements of ions or probes interacting with the ions are sensitive to those ions that are in direct contact with the micelle surface, and single out those as bound. The second type of measurements utilize transport properties like conductivity and ion self-diffusion. The interpretation of these quantities is very complex and is indeed closely connected to our kinetic problem. However, it is not appropriate to discriminate between bound and free ions on the

basis of an electrostatic attraction in excess of  $kT$ , an approximation that has often been used. The third way of determining the degree of binding is by the use of thermodynamic quantities like counterion activity or osmotic coefficient, which is of little interest in the present context.

We will discuss mean first passage times (MFPTs)<sup>15-18</sup> for the diffusion of the quencher ions in the electrostatic field of the charged micelles and their univalent counterions. Formulas for MFPT calculations are given in Appendix B. The methods used to obtain the required numerical solutions of the Poisson-Boltzmann equation for the electrostatic potential are presented briefly in Appendix A. All calculations were made for a spherically symmetrical cell model system as will be described subsequently.

### Cell Model

Cell model theories have been very successful in describing the thermodynamic properties of ionic micelle solutions.<sup>13,19-22</sup>

Each micelle resides in the center of a spherical cell comprising solvent and other constituents so that the composition is the same as that of the total solution. The volume of the spherical cell is likewise determined so that it equals the mean volume available for micelles in the solution. All calculations with the Poisson-Boltzmann equation or of MFPT are confined to one cell, the outside world being represented by appropriate boundary conditions on the cell limit. The total solution may be envisaged as being composed of close-packed spherical cells, neglecting the small voids between the points of contact. It is only a small step to transform this model into one where the nearest-neighbor cells are smeared out (as they will be on average over time). By symmetry reasons the cell boundary will now be an equipotential surface (with zero field strength), and the cell is perfectly spherically symmetrical.

The details, including parameter values, of the model used in the calculations are presented in Appendix C.

### Results from Calculations

**Bound-Free Division.** The mean first passage times for a quencher ion to go from a start position  $r_0$  to the rim of the cell,  $\tau(r_0, r_c)$ , the escape time, and from  $r_0$  to the micelle surface,  $\tau(r_0, r_m)$ , were estimated for several SDS concentrations. Parameter values used are reported in Appendix C. The results for the lowest and highest SDS concentrations are shown in Figures 1 and 2. For a bivalent quencher ion the "binding radius" according to the suggested definition (eq 4) is very close to  $r_c$ . Almost all multivalent ions are bound at both concentrations. For an uncharged species  $r_b$  is instead close to the micelle surface and very few neutral species are bound, which is as it should be in the absence of specific or hydrophobic binding. For the univalent species  $r_b$  is intermediate—this is of course the most problematic case. The fractions of bound quencher ions according to different definitions are compared in Table I.

The MFPTs in Figures 3 and 4 are averages over start positions in  $r_m$ ,  $r_2$  and absorption at  $r_m$ ,  $\tau(r_m, r_2, r_m)$  or  $r_c$ ,  $\tau(r_m, r_2, r_c)$ . The corresponding quantities for start positions in the interval  $r_1, r_c$  are shown in Figures 5 and 6. These results are quite instructive and give further insight into the time scales of the ion movements. Figure 7 presents designations, values, and schematic diagrams for various MFPTs calculated for 2+ ions with a diffusion coefficient of  $5 \times 10^{-10} \text{ m}^2 \text{ s}^{-1}$  ( $\text{Cu}^{2+}$ ). All MFPTs from a bound position to the cell boundary ( $r_c$ ) are virtually equal. This is typical for a situation when the steady-state approximation (SSA) for

(10) Hatlee, M. D.; Kozak, J. J.; Rothenberger, G.; Infelta, P. P.; Grätzel, M. *J. Phys. Chem.* **1980**, *84*, 1508.

(11) Sano, H.; Tachiya, M. *J. Chem. Phys.* **1981**, *75*, 2870.

(12) Gösele, U.; Klein, U. K. A.; Hauser, M. *Chem. Phys. Lett.* **1979**, *68*, 291.

(13) Gunnarsson, G.; Jönsson, B.; Wennerström, H. *J. Phys. Chem.* **1980**, *84*, 3114.

(14) Lindman, B.; Wennerström, H. *Top. Curr. Chem.* **1979**, *87*, 1.

(15) Weiss, G. H. *Adv. Chem. Phys.* **1967**, *13*, 1.

(16) Szabo, A.; Schulten, K.; Schulten, Z. *J. Chem. Phys.* **1980**, *72*, 4350.

(17) Deutch, J. M. *J. Chem. Phys.* **1980**, *73*, 4700.

(18) Schulten, K.; Schulten, Z.; Szabo, A. *J. Chem. Phys.* **1981**, *74*, 4426.

(19) Jönsson, B. Ph.D. Thesis, University of Lund, Sweden, 1981.

(20) Jönsson, B.; Wennerström, H. *J. Colloid Interface Sci.* **1981**, *80*, 482.

(21) Linse, P.; Gunnarsson, G.; Jönsson, B. *J. Phys. Chem.* **1982**, *86*, 413.

(22) Linse, P.; Jönsson, B. *J. Chem. Phys.* **1983**, *78*, 3167.

(23) Gunnarsson, G. Ph.D. Thesis, University of Lund, Sweden, 1981.

(24) Aniansson, G. *J. Phys. Chem.* **1978**, *82*, 2805.

(25) Cabos, C.; Delord, P.; Martin, J. C. *J. Phys. Lett.* **1979**, *40*, 407.

(26) Ise, N.; Okubo, T. *Acc. Chem. Res.* **1980**, *13*, 303.

TABLE I: Fraction of Quencher Ions Classified as Bound According to Some Definitions

$z$	$C_{\text{SDS}}$ , mM	$r_c$ , Å	$r_b$ , Å	fraction of $M^{z+}$ ions with		
				$r < r_m + 3 \text{ Å}$	$ ze\Psi(r) /kT < 1$	$r < r_b$
2 <sup>+</sup> <sup>a</sup>	25	107.6	107.1	0.93	0.99	0.99996
2 <sup>+</sup> <sup>a</sup>	300	45.5	45.3	0.92	0.99	0.9998
1 <sup>+</sup> <sup>b</sup>	25	107.6	75.5	0.35	0.58 (43.8 Å)	0.74
1 <sup>+</sup> <sup>b</sup>	300	45.5	41.8	0.49	0.70 (29.6 Å)	0.93
1 <sup>+</sup> <sup>a</sup>	25	107.6		0.29	0.51	
1 <sup>+</sup> <sup>a</sup>	300	45.5		0.49	0.69	

<sup>a</sup> Calculated with  $[M^{z+}] = 1.00 \text{ mM}$ . <sup>b</sup> Calculated with  $[M^{z+}] = 0$ .

TABLE II: Mean First Passage Times for Uncharged and Positively Charged Particles in the Potentials of SDS Micelles

MFPT <sup>a</sup>	$C_{\text{SDS}} =$	$10^{10} D \tau / \text{m}^2$					
		$z = 2$		$z = 1$		$z = 0$	
		25 mM	300 mM	25 mM	300 mM	25 mM	300 mM
$\tau(r_m, r_c)$		$1.2 \times 10^6$	$1.5 \times 10^4$	$9.0 \times 10^3$	$8.1 \times 10^2$	$1.8 \times 10^3$	$1.9 \times 10^2$
$\tau(r_m, r_b, r_c)$		$1.2 \times 10^6$	$1.5 \times 10^4$	$8.1 \times 10^3$	$7.2 \times 10^2$	$1.8 \times 10^3$	$1.9 \times 10^2$
$\tau(r_m, r_c, r_c)$		$1.2 \times 10^6$	$1.5 \times 10^4$	$6.4 \times 10^3$	$6.8 \times 10^2$	$7.5 \times 10^2$	97
$\tau(r_m, r_b, r_b)$		$1.2 \times 10^6$	$1.5 \times 10^4$	$4.7 \times 10^3$	$5.4 \times 10^2$	1.2	3.7
$\tau(r_m, r_r, r_r)$	25	22		7.4		2.6	2.6
$\tau(r_c, r_m)$		$2.5 \times 10^3$	$1.2 \times 10^2$	$4.1 \times 10^3$	$1.9 \times 10^2$	$1.5 \times 10^4$	$5.1 \times 10^2$
$\tau(r_b, r_c, r_m)$		$2.5 \times 10^3$	$1.2 \times 10^2$	$3.9 \times 10^3$	$1.9 \times 10^2$	$1.4 \times 10^4$	$4.4 \times 10^2$
$\tau(r_m, r_c, r_m)$		7.7	2.5	$1.5 \times 10^3$	54	$1.4 \times 10^4$	$4.2 \times 10^2$
$\tau(r_m, r_b, r_m)$		7.9	2.5	$6.5 \times 10^2$	43	$1.0 \times 10^3$	$1.0 \times 10^2$
$\tau(r_b, r_c, r_c)$		$3.3 \times 10^3$	$1.1 \times 10^2$	$1.5 \times 10^3$	87	$7.5 \times 10^2$	91

<sup>a</sup> In  $\tau(r_0, r_a)$   $r_0$  is the start position and  $r_a$  the absorbing boundary. A hard reflecting boundary is placed at  $r = r_c$  when  $r_0 \leq r_0$  and at  $r = r_m$  when  $r_0 > r_0$ .  $\tau(r_1, r_2, r_a)$  denotes  $\tau(r_0, r_a)$  averaged over the equilibrium distribution in the region  $r_1 \leq r_0 \leq r_2$ . The values of  $r_m$  and  $r_c$  were 20 and 107.6 Å at 25 mM SDS, 21.4, and 45.5 Å at 300 mM SDS.  $r_r$  is always  $r_m + 3 \text{ Å}$ .  $r_b = 107.1$  and 45.3 Å for  $z = 2$  at the two concentrations, 75.5 and 41.8 Å for  $z = 1$ , and 22.0 and 25.0 Å at  $z = 0$ .

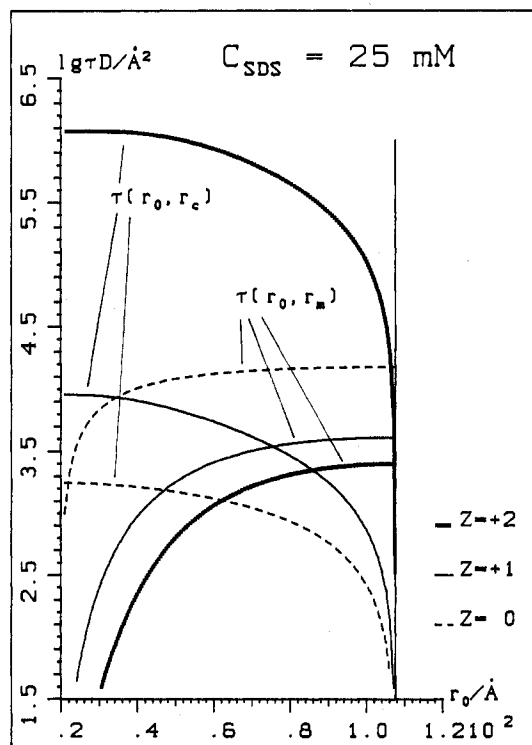


Figure 1. Mean first passage times  $\tau(r_0, r_c)$  and  $\tau(r_0, r_m)$  from a start position  $r_0$  to the cell boundary,  $r_c$ , and to the micelle surface,  $r_m$ . The vertical scale gives the decimal logarithm of the product of  $\tau$  and the diffusion constant of the free ion,  $D$ , the product given in  $\text{Å}^2$ .  $z = 0, 1, 2$  is the charge number of the quencher. Total concentration of SDS,  $C_{\text{SDS}} = 25 \text{ mM}$ .

the MFPT is valid, and a justification for the use of this approximation in the previous calculation.<sup>9</sup> The inward movement of the free ions, which for 2+ ions are only those very close to the rim of the cell, is, of course, much faster than the escape, but still slow compared to the inward movement of bound ions. Since

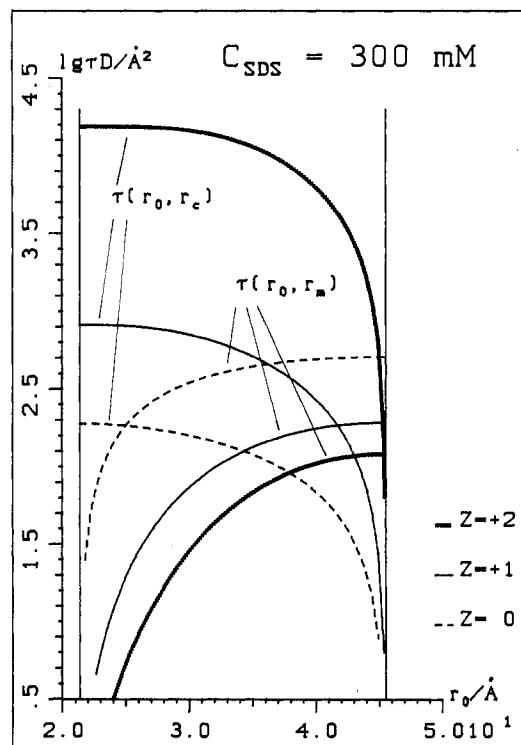


Figure 2. Same as Figure 1, but  $C_{\text{SDS}} = 300 \text{ mM}$ .

the region where a 2+ ion is free is so extremely small, the time that it spends as free is very short, 1.7 ps in the example of Figure 7. It is noteworthy that the MFPT for a free ion to go to  $r_c$  is much longer, 66 ns, which of course is due to the fact that those ions that first cross  $r_b$  and become bound will require a very long time to return.

The situation changes dramatically for  $z = 1+$  and neutral particles, as seen from Table II. Also the SDS concentration has a profound influence.

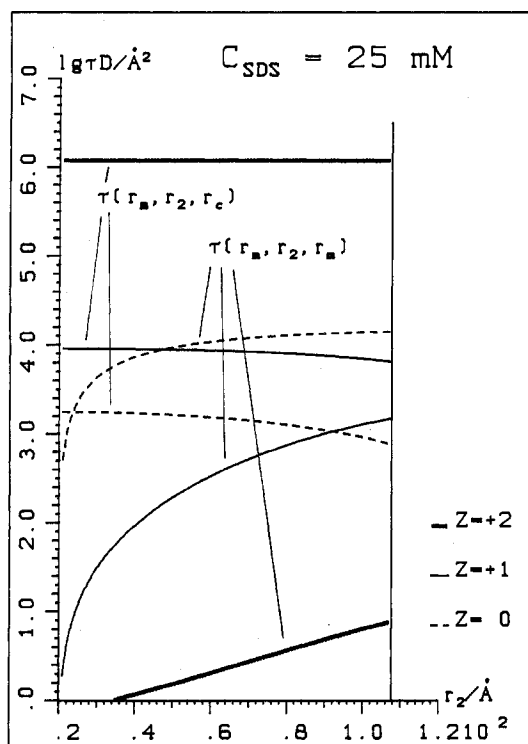


Figure 3. MFPT averaged over start positions in the interval  $r_m \leq r_0 \leq r_2$ .  $\tau(r_m, r_2, r_c)$  denotes the MFPT to reach the cell surface and  $\tau(r_m, r_2, r_m)$  the MFPT to reach the micelle surface.  $C_{\text{SDS}} = 25$  mM.

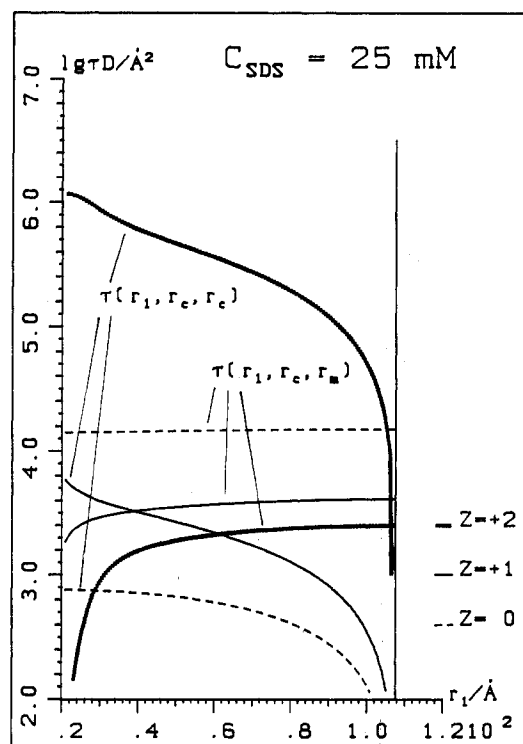


Figure 5. MFPT averaged over start positions in the interval  $r_1 \leq r_0 \leq r_c$ .  $\tau(r_1, r_c, r_c)$  denotes the MFPT to reach the cell surface and  $\tau(r_1, r_c, r_m)$  the MFPT to reach the micelle surface.  $C_{\text{SDS}} = 25$  mM.

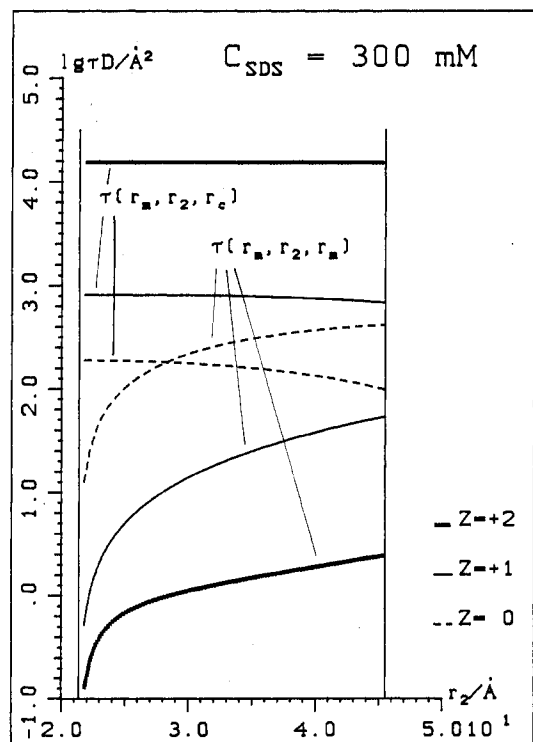


Figure 4. Same as Figure 3, but  $C_{\text{SDS}} = 300$  mM.

For bound 1+ ions the MFPT for going to the cell limit varies strongly with start position. Such a variation is also found for neutral particles (the equality between  $\tau(r_m, r_c)$  and  $\tau(r_m, r_b, r_c)$  is in this case due to the fact that  $r_b$  is very close to  $r_m$ ). The potential well is not deep enough to make the steady-state approximation valid.

The MFPT in the innermost 3 Å thick layer,  $r_m$  to  $r_r$ , for leaving the reaction zone,  $\tau(r_m, r_r, r_r)$ , is almost concentration independent, which is a consequence of the often noted fact that the electrostatic

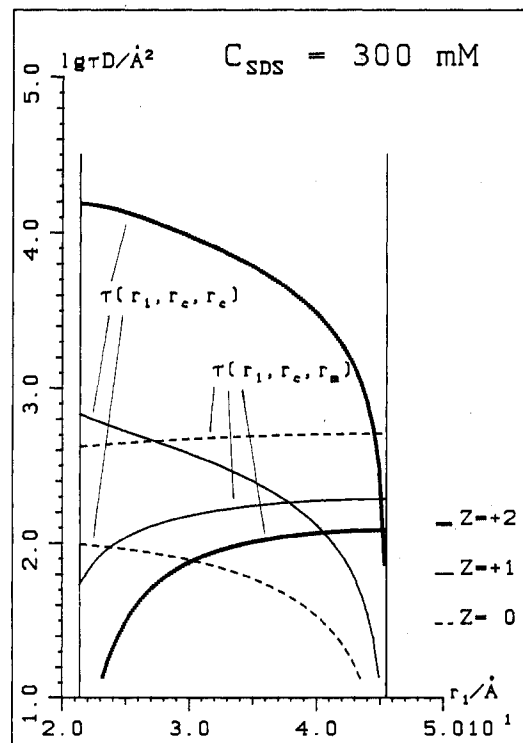
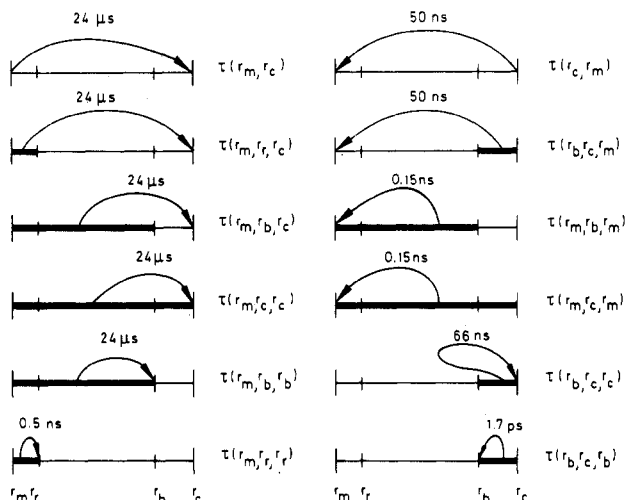


Figure 6. Same as Figure 5, but  $C_{\text{SDS}} = 300$  mM.

ion binding, and the electric forces, close to the surface are quite insensitive to changes in concentration of micelles and also salt.<sup>22</sup>

Some other aspects that are more directly related to the free-bound concepts may be noted. For particles classified as bound Table II shows that the ratios of the MFPTs for going to the cell rim and to the micelle surface are about  $10^5$  ( $10^4$ ) for  $z = 2+$  at 25 mM (300 mM), 13 (17) for  $z = 1+$ , and less than 2 for neutral species. A free ion goes to the cell boundary much more rapidly than a bound one, by a factor of 450 at 25 mM SDS and  $z = 2+$ ,



**Figure 7.** Values, designations, and schematic diagrams over mean first passage times calculated for  $2+$  ions with  $D = 5 \times 10^{-10} \text{ m}^2 \text{ s}^{-1}$  in the Poisson-Boltzmann potential of SDS micelles at a concentration of 25 mM. The micelle radius  $r_m = 20 \text{ \AA}$ , reaction-zone radius  $r_r = 23 \text{ \AA}$ , bound-ion radius according to suggested definition  $r_b = 107.1 \text{ \AA}$ , and cell radius  $r_c = 107.6 \text{ \AA}$ .

and by a factor of 5–10 at  $z = 1+$ .

These results suggest that the bound-free division according to eq 4 works very well for multivalent ions—where in effect all may be regarded as bound. The neutral particles are, of course, not bound electrostatically.

The absolute values of  $D\tau$  in Table II are of some interest. A free diffusion in two dimensions as on the micelle surface gives a mean square diffusion length of  $2(D\tau)^{1/2}$ . Only if the bound ion stays so long with the micelle that it may diffuse around it will the point of exit from the bound region be uncorrelated to the entrance point. The requirement may be stated as

$$D\tau \gg \pi^2 r_m^2 \approx 4000 \text{ \AA}^2$$

The bivalent ions fulfill this criterion at both 25 and 300 mM SDS and the univalent ions at 25 mM. At high micelle concentration, however, a univalent counterion will not stay long enough with a micelle to lose the memory of the point of entrance. The probability of encounter with a target at the micelle surface on a single visit is also considerably less than unity. The model situation described in the Introduction does not apply to the univalent quencher ions, therefore. The experimentally registered fluorescence decay curves show only small deviations from exponentiality,<sup>7,8</sup> and not the distinct two-phasic behavior.

**Rate Constants.** It was remarked above that the binding of ions very close to the charged surface has been observed and predicted to be rather insensitive to changes in micelle and salt concentration. An implication is that  $k_q$  from eq 5 would be equally insensitive to concentration changes and would be a good rate constant, therefore.

The constant  $k_-$  has been discussed above as the inverse mean residence time of bound ions. For multivalent ions it is in practice the residence time in a cell. The measurement of the amplitude and the decay constant of the steady-state portion will not provide any direct information on  $k_q$  and  $k_-$  as long as the latter is much smaller than the former (if not, the model breaks down). If the rate of diffusional arrival of new quenchers to the cell in the steady-state phase of the decay equals the equilibrium rate of entrance into the cell, then the decay constant of the exponential final decay phase should be  $k_- \langle x \rangle$ , where  $\langle x \rangle$  is simply the ratio of quencher ion concentration to micelle concentration (all the multivalent ions are bound) and  $k_-$  the inverse of the residence time in the cell. Since an ion at the very cell limit has about equal chance to proceed or return, the residence time in the cell should be about twice the mean first passage time to the cell limit. Thus, for multivalent quenchers

$$(k_-)^{-1} = 2\tau(r_m, r_c, r_c) \quad (6)$$

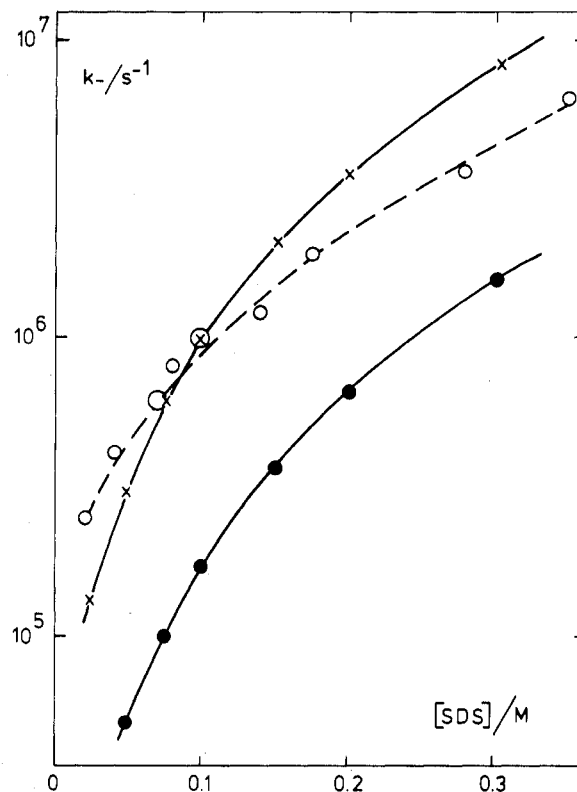


**Figure 8.** Calculated (X, ●) and experimental (O) values of the escape rate constant  $k_-$  for  $\text{Cu}^{2+}$  at different total SDS concentrations. The two sets of calculated values differ only in that the radius of closest approach of the  $\text{Cu}^{2+}$  ions has been taken as equal to the radius of closest approach of  $\text{Na}^+$  in one case (●) and  $1.5 \text{ \AA}$  larger than that in the other (X).

The steady-state approximation will be good for the calculation of the MFPT in this case (Appendix B).

**Comparison of Numerical and Experimental Results for  $\text{Cu}^{2+}$  Quenching in SDS.** Experimental values for  $k_-$  were obtained as follows. The values of parameters  $A_1$ – $A_4$  in eq 1 were determined as described earlier.<sup>7</sup> With  $k_q \gg k_-$  and  $k_0$  known one gets for each micelle concentration

$$k_- = (A_2 - k_0) / A_3 \quad (7)$$

A check on  $A_3 = \langle x \rangle$  is obtained from the known values of micelle size, concentration of quencher (all bound), and concentration of surfactant in micellar form.

The results for  $k_-$  from the quenching of methylpyrene by  $\text{Cu}^{2+}$  ions in SDS<sup>27</sup> at concentrations up to 0.35 M are shown in Figure 8, together with two sets of results from numerical calculations, differing in that  $\text{Cu}^{2+}$  and  $\text{Na}^+$  in one case were allowed to approach equally close to the micelle surface, whereas in the other the closest approach of  $\text{Cu}^{2+}$  was  $1.5 \text{ \AA}$  further out. A somewhat lower value of this radius of closest approach would have given a better agreement with the experimental finding at high concentrations of SDS, but still be a factor of 2 off or more at the lowest SDS concentration. An important aspect of the results is the enormous difference between the two sets of calculated values. It shows that the potential curve close to the micelle surface is very important. The calculations are based on a smooth micelle surface with a continuous charge density. In reality the charges are localized and the surface probably rough with dynamically protruding head groups.<sup>24</sup> Aniansson's calculations<sup>24</sup> suggest that the surface roughness and protruding charges result in a less steep potential curve close to the surface and to a smaller overall potential change than in the smooth interface model and, as a consequence, a faster migration of counterions.

In view of this the absolute values calculated for the rate constant  $k_-$  should not be regarded with much confidence, but

(27) Croonen, Y. Ph.D. Thesis, Katholieke Universiteit Leuven, Belgium, in preparation.

the variation of the values with the micelle concentration should be more reliable. From Figure 8 it is evident that the calculated values decrease too quickly at low SDS concentrations. In this connection one of the shortcomings of the cell model may be important. The micelles are regarded as stationary, each at the midpoint of its cell. Although a certain long-range ordering is apparent both from X-ray and neutron scattering experiments<sup>25,26</sup> and from Monte Carlo calculations,<sup>22</sup> the micelles are in motion and spend much time appreciably closer together than at the mean separation, in particular when the concentration is low. These micelle approaches will contribute to a quicker ion exchange, a mechanism reminiscent of the "hopping mechanism" first suggested by Henglein et al.<sup>28</sup> in a somewhat different context.

The results of the present calculations are quite close to those presented earlier,<sup>9</sup> although a number of improvements were inserted; the most important may be the factor of 2 in the expression for  $(k_-)^{-1}$ . Furthermore, the mean first passage time was previously calculated in the steady-state approximation but now exactly. It was remarked above that the steady-state approximation is very good for the 2+ ions even at the highest micelle concentration, but rather poor for univalent ions. The present calculations also took account of the changes in the free-monomer concentration and in the micelle aggregation number—the latter as assessed by fluorescence quenching measurements.<sup>4</sup> The effects of these refinements were rather small. The need for a detailed description of the electrostatics and dynamics at the micelle surface remains an unsurmountable obstacle for more realistic calculations at present.

### Concluding Remarks

The conclusion concerning the proposed definition of bound and free ions must be that it works fine for multivalent ions and neutral species but is unnecessary in those cases because either almost all or almost none of the species are bound. The definition yields a much more interesting result when applied to univalent species, but the value of the definition in that case remains to be proven. It is probably difficult to get a good test from quenching kinetics, because the residence time of the univalent ion with the micelle is short already at low micelle concentrations, and the rate constant of quenching will never be much larger than the escape rate constant. Under such conditions the fluorescence decay will be close to exponential, and the estimates of the parameter values in a rate law such as eq 1 will be rather uncertain.

### Appendix A

**Poisson-Boltzmann Equation and Its Numerical Solution.** *Poisson-Boltzmann Equation.* The distribution of charged particles in a finite region is commonly obtained by means of the Poisson-Boltzmann (PB) equation.<sup>13,29-33</sup> From the distributions other mechanical and thermodynamic quantities can easily be calculated. The PB equation can rigorously be derived from the primitive model. In the primitive model of systems containing charged particles, the interaction potential  $U_{ij}(r)$  between the mobile charged particles  $i$  and  $j$  separated by a distance  $r$  is

$$U_{ij}(r) = e^2 z_i z_j / (4\pi\epsilon_0\epsilon_r r) \quad r \geq R_i + R_j \\ = \infty \quad r < R_i + R_j \quad (\text{A1})$$

where  $ez_i$  and  $ez_j$  are the charges of the particles,  $\epsilon_0\epsilon_r$  the dielectric permittivity, and  $R_i$  and  $R_j$  the hard-core radius of the particles. The interaction potential between a mobile particle  $i$  and a fixed particle (in our case the micelle) is given by

$$U_i(r) = ez_i \Psi_m(r) \quad r \geq R_i + R_m \\ = \infty \quad r < R_i + R_m \quad (\text{A2})$$

where  $\Psi$  is the electrostatic potential arising from the micelle. Now by introducing the following two approximations, one may derive the PB equation:<sup>34</sup> (i) The radius of mobile particle  $i$ ,  $R_i$ , is zero. (ii) The pair correlation function  $g_{ij}$  between the mobile ions  $i$  and  $j$  is constant and unity.

The results of the PB equation agree satisfactorily with results from exact statistical mechanics solution of a system modeling micellar solution in the primitive model with monovalent counterions.<sup>21,22</sup> However, at a concentration of divalent counterions of 1–10 mM the PB equation breaks down.<sup>21,22</sup> The concentration limit depends on micelle concentration, micelle charge, concentration of monovalent counterions, and the quantity of interest.

**Numerical Solution.** The PB equation may be written as

$$\epsilon_0\epsilon_r \nabla^2 \Psi = \sum_i z_i e c_{i0} \exp(-z_i e \Psi / kT) \quad (\text{A3})$$

where  $\Psi$  is the mean electrostatic potential,  $c_{i0}$  the concentration of the mobile particle  $i$  at zero electrostatic potential,  $k$  the Boltzmann constant, and  $T$  the absolute temperature. In the calculations, the potential is chosen so that

$$\Psi(r_c) = 0 \quad (\text{A4})$$

where  $r_c$  is the radius of the spherical cell. This is possible since the absolute value of the potential for an electroneutral system is arbitrary. The other boundary conditions of eq A3 are

$$\Psi'(r)|_{r=r_c} = 0 \quad (\text{A5})$$

by symmetry and

$$\Psi'(r)|_{r=r_m} = -\sigma / (\epsilon_0\epsilon_r) \quad (\text{A6})$$

since the total system is electroneutral. Here  $\sigma$  is the surface charge density of the micelle. The last boundary condition is

$$c_{i0} \int_{r_m}^{r_c} dr 4\pi r^2 \exp(-z_i e \Psi / kT) = V' \bar{c}_i \quad (\text{A7})$$

$$i = 1, 2, \dots, n$$

$$V' = (4\pi/3)r_c^3 \quad (\text{A8})$$

which relate the mean concentration of the  $n$  ionic species  $\bar{c}_i$ ,  $i = 1, 2, \dots, n$ , with  $\Psi(r)$  and  $c_{i0}$ ,  $i = 1, 2, \dots, n$ . One of the  $n+1$  relations from eq A6 and A7 is linearly dependent on the others and we will restrict ourselves to  $i = 2, 3, \dots, n$  in eq A7.

By introduction of the reduced quantities

$$x = r/r_c \quad (\text{A9})$$

$$\phi = e\Psi/kT \quad (\text{A10})$$

eq A3–A8 are transformed into

$$\frac{d^2\phi}{dx^2} + \frac{2}{x} \frac{d\phi}{dx} = \frac{e^2}{\epsilon_0\epsilon_r kT} r_c^2 \sum_i z_i c_{i0} \exp(-z_i \phi) \quad (\text{A3}')$$

$$\phi(1) = 0 \quad (\text{A4}')$$

$$\left. \frac{d\phi}{dx} \right|_{x=1} = 0 \quad (\text{A5}')$$

$$\left. \frac{d\phi}{dx} \right|_{x=\xi} = -\frac{\sigma}{\epsilon_0\epsilon_r} \frac{e}{kT} r_c \quad \xi = r_m/r_c \quad (\text{A6}')$$

$$c_{i0} \int_{\xi}^1 dx 4\pi x^2 \exp(-z_i \phi) = (4\pi/3) \bar{c}_i \quad (\text{A7}')$$

$$i = 2, 3, \dots, n$$

In order to solve the set of equations A3'–A7', we need start values of  $c_{i0}$ ,  $i = 1, 2, 3, \dots, n$ . These values are used together with eq A4' and A5' to solve eq A3'.

(34) Jönsson, B.; Wennerström, H.; Halle, B. *J. Phys. Chem.* **1980**, *84*, 2179.

(28) Henglein, A.; Proske, Th. *Ber. Bunsenges. Phys. Chem.* **1978**, *82*, 471.  
 (29) Jönsson, B.; Wennerström, H. *Chem. Scr.* **1980**, *15*, 40.  
 (30) Fuoss, R.; Katchalsky, A.; Lifson, S. *Proc. Natl. Acad. Sci. U.S.A.*, **1951**, *37*, 579.  
 (31) Alfrey, I.; Berg, P. W.; Morawetz, H. *J. Polym. Sci.* **1951**, *7*, 543.  
 (32) Bell, G. M.; Dunning, A. J. *Trans. Faraday Soc.* **1970**, *66*, 500.  
 (33) Mille, M.; Vanderkooi, G. *J. Colloid Interface Sci.* **1977**, *59*, 211.

Runge-Kutta method with variable step length until  $\phi'(x^{(1)}) = \phi'(\xi)$ . However,  $x^{(1)}$  and  $\bar{c}_i^{(1)}$ ,  $i = 2, 3, \dots, n$ , from eq A7' will generally differ from  $\xi$  and  $\bar{c}_i$ ,  $i = 2, 3, \dots, n$ , which is the desired solution. The Jacobian

$$d(x, \bar{c}_i)/d(c_{j0}) \quad (\text{A9}')$$

$$i = 2, 3, \dots, n \quad j = 1, 2, \dots, n$$

around  $x^{(1)}$  and  $\bar{c}_i^{(1)}$ ,  $i = 2, 3, \dots, n$ , is now calculated. By means of a  $n$ -dimensional Newton-Raphson iteration, we obtain new values of  $c_{j0}$ ,  $j = 1, 2, \dots, n$ , and these are used to solve eq A3' again. The iteration proceeds until the desired accuracy of  $\xi$  and  $\bar{c}_i$ ,  $i = 2, 3, \dots, n$ , is achieved.

## Appendix B

**Mean First Passage Time.** The mean first passage time (MFPT) or its inverse, an escape rate constant, is a one-parameter description of the time evolution of a diffusion-controlled process. These MFPTs can be evaluated numerically from the electrostatic potential obtained in the continuum model. Here we will merely give the equations used to calculate the MFPTs and leave the general discussion to ref 15-18 and 35.

The mean first passage times for a diffusing particle to go from a start position  $r_0$  to  $r_a$  will be denoted  $\tau(r_0, r_a)$ . In spherical symmetry,  $\tau(r_0, r_a)$  is given by

$$\tau(r_0, r_a) = \int_{r_0}^{r_a} dx \frac{x^{-2}}{D(x)} \exp(z\phi) \int_{r_c}^x dy y^2 \exp(-z\phi) \quad (\text{B1})$$

$$r_a \leq r_0$$

$$\tau(r_0, r_a) = \int_{r_0}^{r_a} dx \frac{x^{-2}}{D(x)} \exp(z\phi) \int_{r_m}^x dy y^2 \exp(-z\phi) \quad (\text{B2})$$

$$r_a \geq r_0$$

where  $r_m$  is the micelle radius,  $r_c$  the cell radius,  $D(x)$  the space-dependent diffusion constant,  $z$  the valency of the particle, and  $\phi$  the reduced electrostatic potential. A hard reflecting wall is placed at  $r = r_c$  when  $r_a \leq r_0$  and at  $r = r_m$  when  $r_a > r_0$ . In our application, we will consider  $D(x)$  independent of position.

We are also interested in MFPTs averaged over the equilibrium distribution of the particle in a region  $r_1 \leq r_0 \leq r_2$ . These quantities will be denoted  $\tau(r_1, r_2, r_a)$ . Following Szabo et al.,<sup>16</sup>  $\tau(r_1, r_2, r_a)$  may be expressed by

$$\tau(r_1, r_2, r_a) = \left\{ \int_{r_1}^{r_2} dx x^2 \exp(-z\phi) \right\}^{-1} \int_{r_1}^{r_2} dr_0 r_0^2 \exp(-z\phi) \tau(r_0, r_a) \quad (\text{B3})$$

In the case that  $r_1 = r_a = r_m$  and  $r_2 = r_c$  and by means of eq B1, eq B3 can be written

$$\tau(r_m, r_c, r_m) = \left\{ \int_{r_m}^{r_c} dx x^2 \exp(-z\phi) \right\}^{-1} \int_{r_m}^{r_c} dx \frac{x^{-2}}{D(x)} \times \exp(z\phi) \left\{ \int_x^{r_c} dy y^2 \exp(-z\phi) \right\}^2 \quad (\text{B4})$$

When  $r_1 = r_m$  and  $r_2 = r_a = r_c$  one obtains

$$\tau(r_m, r_c, r_c) = \left\{ \int_{r_m}^{r_c} dx x^2 \exp(-z\phi) \right\}^{-1} \int_{r_m}^{r_c} dx \frac{x^{-2}}{D(x)} \times \exp(z\phi) \left\{ \int_{r_m}^x dy y^2 \exp(-z\phi) \right\}^2 \quad (\text{B5})$$

If  $(r_1, r_2) \neq (r_m, r_c)$ , equations corresponding to eq B4 and B5 are not so simple. We have used eq B3 to average  $\tau(r_0, r_a)$  over the interval  $r_1$ - $r_2$  in all cases and, when  $(r_1, r_2) = (r_m, r_c)$ ,  $r_a = r_m$ , or  $r_a = r_c$ , we have checked our solution against eq B4 and B5.

The steady-state approximation (SSA) can be used when the escape over a high barrier from a potential well is considered.<sup>18</sup> The probability density in the well is assumed to be at quasi-

TABLE III: Data of Concentration of Free Amphiphile [SDS], Aggregation Number  $n$ , Micelle Radius  $r_m$ , and Cell Radius  $r_c$  at Different Total SDS Concentrations,  $C_{\text{SDS}}$

$C_{\text{SDS}}$ , mM	[SDS], <sup>a</sup> mM	$n^b$	$r_m$ , <sup>c</sup> Å	$r_c$ , Å
15	6.4	62	20.0	141.9
25	5.3	62	20.0	107.6
50	3.8	63	20.2	81.5
75	3.0	63	20.2	70.3
100	2.5	64	20.3	63.8
150	2.0	65	20.5	55.8
200	1.7	67	20.8	51.2
300	1.4	71	21.4	45.5

<sup>a</sup> Reference 13. <sup>b</sup> Reference 4. <sup>c</sup> Assuming constant surface charge density (see text).

equilibrium. The escape becomes a simple exponential function of time, characterized by the MFPT in the SSA,  $\tau_{\text{SS}}$ . With  $r_a = r_c$  the SSA of eq B2 is

$$\tau_{\text{SS}} = \int_{r_m}^{r_c} dx \frac{x^{-2}}{D(x)} \exp(\exp(z\phi)) \int_{r_m}^{r_c} dx x^2 \exp(-z\phi) \quad (\text{B6})$$

independent of start position.

## Appendix C

**Model of the Micelle Solution.** The Poisson-Boltzmann equation was solved at a temperature  $T = 298$  K and with a relative dielectric permittivity  $\epsilon_r = 78.3$ . The concentration of free amphiphile in the solution was taken from the model of Gunnarsson et al.,<sup>13</sup> which gives a decreasing amphiphile activity at an increasing total amphiphile concentration. The values of free amphiphile concentration used are given in Table III and are calculated in the salt-free case. The aggregation number,  $n$ , increases slightly with the total amphiphile concentration,  $c_A$ . The micellar radius  $r_m$  was calculated by keeping the surface charge density fixed,  $\sigma = -0.976$  C m<sup>-2</sup>. The micelle radius  $r_m$  and the cell radius  $r_c$  are also given in Table III.

In order to make a more accurate model, we have to consider how the presence of divalent counterions affects the concentration of free amphiphiles (the influence from the co-ions can be neglected). Unfortunately the activity of the amphiphile in the presence of added salt is not very well-known experimentally. However, Fisher et al.<sup>36</sup> and Newbury<sup>37</sup> have recently measured how the cmc of SDS decreases upon the addition of Ni(NO<sub>3</sub>)<sub>2</sub>. At [Ni<sup>2+</sup>] = 1.0 mM, Newbury gives a cmc of 2.2 mM, as compared to 8.0 mM without salt. The concentration of free amphiphile at higher total amphiphile concentration should also decrease in the presence of added salt. Thus, at [SDS] = 25 mM and [Ni<sup>2+</sup>] = 1.0 mM the concentration of free amphiphile ought to be well below 5.3 mM. To see how the presence of M<sup>2+</sup> and free amphiphiles affects the potential and the MFPTs, we have considered three cases with  $C_{\text{SDS}} = 25$  mM: (a) [SDS] = 5.3 mM, [M<sup>2+</sup>] = 0.0 mM; (b) [SDS] = 5.3 mM, [M<sup>2+</sup>] = 1.0 mM; (c) [SDS] = 0.0 mM, [M<sup>2+</sup>] = 1.0 mM. In these calculations, we have neglected the influence of the divalent counterions upon the aggregation number, which is small at [M<sup>2+</sup>] = 1.0 mM.<sup>4,38</sup> The corresponding reduced electrostatic potentials at the micelle surface are -6.7, -6.4, and -6.8, respectively. The maximal deviation of any MFPT studied in case b from MFPT in case a is a factor of 2 and between cases a and c 15%, now in the opposite direction.

Since the presence of M<sup>2+</sup> and the thereby induced decrease in free-SDS concentration have counteracting effects on the potential and the MFPT, and since the concentration of free SDS is uncertain, we have chosen a model according to the case a and Table III. Thus, if nothing else is stated, the calculations are based on the assumption that the divalent counterions affect neither the micellar size nor the distribution of counterions and amphiphiles.

(36) Fischer, M.; Knoche, W.; Robinson, B. H.; Wedderburn, J. H. M. *J. Chem. Soc., Faraday Trans. 1* 1979, 75, 119.

(37) Newbury, J. E. *J. Colloid Interface Sci.* 1980, 74, 483.

(38) Almgren, M.; Swarup, S. *J. Phys. Chem.* 1983, 87, 876.